Int. J. Heat Mass Transfer. Vol. 5, pp. 1111–1115. Pergamon Press 1962. Printed in Great Britain.

SHORTER COMMUNICATION

ABSORPTION OF THERMAL RADIATION IN A V-GROOVE CAVITY

E. M. SPARROW and S. H. LIN
Heat Transfer Laboratory, University of Minnesota

INTRODUCTION

THIS paper is concerned with the energy absorbed when radiation from an external source enters a V-groove cavity. Consideration is given to cavities whose surfaces are either diffuse reflectors or specular reflectors. For each one of these surface conditions, two general types of incoming radiation are studied: (a) energy arriving in a bundle of parallel rays, (b) energy diffusely streaming in through the cavity opening.

PARALLEL RAYS, DIFFUSE SURFACES

Fully illuminated surfaces, $\gamma < \frac{1}{2}\theta$

The analysis is facilitated by reference to Fig. 1(a), from which it is seen that both surfaces are directly illuminated by the incoming rays when $\gamma < \frac{1}{2}\theta$. The rate at which energy is carried by the incoming stream is denoted by S per unit area normal to the ray. The energy H locally incident per unit time and area is the sum of the direct illumination plus the radiation reflected from the other surface locations. Thus

$$H(x) = S\sin\left(\frac{\theta}{2}+\gamma\right) + \rho\int_{y=0}^{L} H(y)\,dF_{x-y}$$

$$H(y) = S\sin\left(\frac{\theta}{2}-\gamma\right) + \rho\int_{x=0}^{L} H(x)\,dF_{y-x} \quad (1)$$

in which the diffuse angle factors dF_{x-y} and dF_{y-x} are available from [1]. The reflectivity ρ and absorptivity α are related by $\rho = (1-\alpha)$. Because of the linearity of the integral equations (1), their solution can be constructed by superposing solutions of the alternate pair of dimensionless integral equations

$$f(\xi) = \alpha + \rho\int_0^1 g(\eta)\,dF_{\xi-\eta}, \quad g(\eta) = \rho\int_0^1 f(\xi)\,dF_{\eta-\xi}. \quad (2)$$

Once the solution for H has been obtained, the rate q at which energy is locally absorbed per unit time and area is found simply by writing $q = \alpha H$. Utilizing the superposition noted above,

$$q(x)/S = f(x/L)\sin\left(\frac{\theta}{2}+\gamma\right) + g(x/L)\sin\left(\frac{\theta}{2}-\gamma\right) \quad (3a)$$

$$q(y)/S = f(y/L)\sin\left(\frac{\theta}{2}-\gamma\right) + g(y/L)\sin\left(\frac{\theta}{2}+\gamma\right). \quad (3b)$$

The total rate Q at which energy is absorbed in the cavity (unit dimension normal to page) is obtained by integrating $q(x)\,dx$ and $q(y)\,dy$. It is convenient to represent the results for Q in terms of an apparent absorptivity α_a defined as

$$\alpha_a = (\text{total absorbed energy})/(\text{total incoming energy}). \quad (4)$$

For the case of parallel rays, the total rate of incoming energy is $(S\cos\gamma)[2L\sin(\theta/2)]$. Then, integrating equations (3a) and (3b) and utilizing the definition (4), there follows

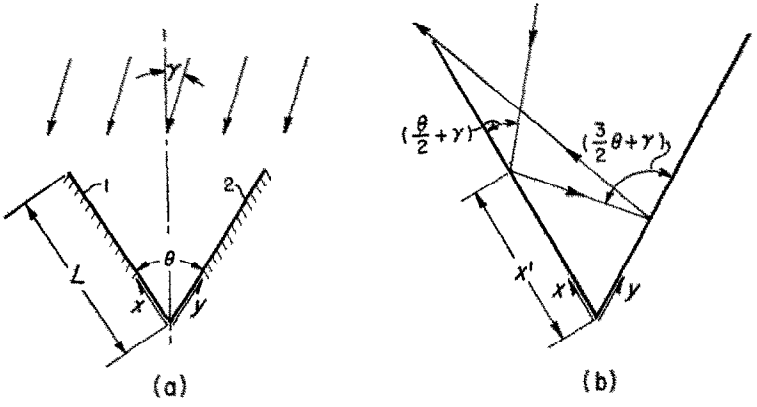

FIG. 1. Diagrams for absorption analysis for parallel-ray bundle.

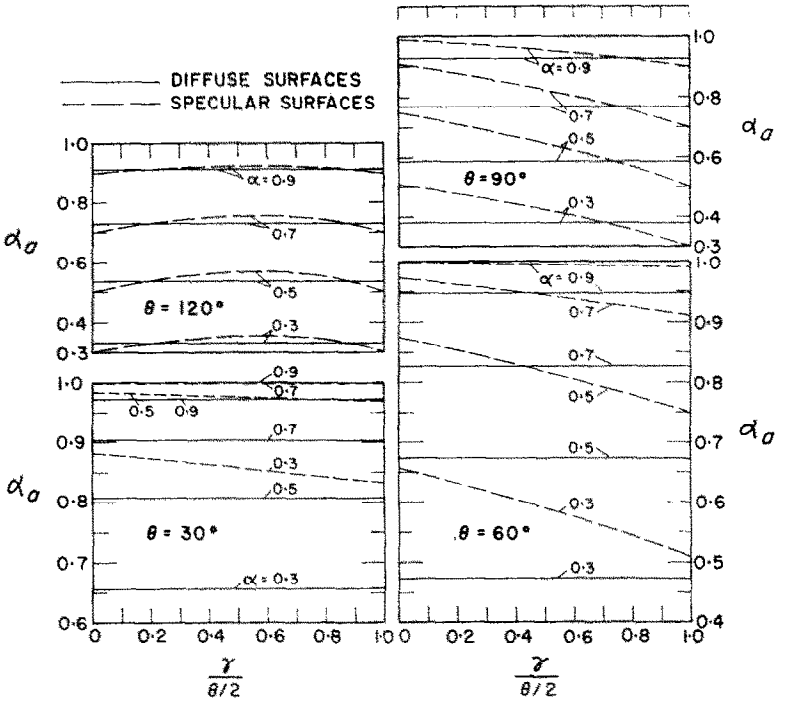

FIG. 2. Apparent absorptivity for parallel rays incident on a V-groove, $\gamma \leqslant \theta/2$.

$$a_a = \int_0^1 f(\xi)\,\mathrm{d}\xi + \int_0^1 g(\eta)\,\mathrm{d}\eta. \qquad (5)$$

Numerical solutions of equations (2) have been carried out on a Univac 1103 electronic computer for opening angles θ of 30°, 60°, 90° and 120°, and for surface absorptivity values α of 0·3, 0·5, 0·7 and 0·9. Utilizing these, the apparent absorptivity of the cavity has been evaluated from equation (5) and the results plotted on Fig. 2 as solid lines. From the figure, it is seen that in all cases a_a exceeds α, and the extent of this deviation is a measure of the cavity effect (i.e. the multireflections within the cavity). Further inspection of the figure reveals that deviations of a_a from α are most marked for cavities of small opening angle and small surface absorptivity. Also, a_a is independent of γ, when $\gamma < \frac{1}{2}\theta$.

The detailed distributions of the functions f and g are needed for the computation of the local heat transfer in equations (3a) and (3b). Space limitations preclude presentation of all the f and g functions which have been calculated. Typical distributions are presented in Figs. 3 and 4, which correspond respectively to $\theta = 30°$ and 120°. In conjunction with equations (3), these figures show that the greatest energy absorption takes place near the apex (near $x = 0$) for the condition $\gamma < \frac{1}{2}\theta$. Also, the energy absorption is less uniform at smaller opening angles.

Partially illuminated surfaces, $\gamma > \frac{1}{2}\theta$

By referring to Fig. 1(a), it is seen that, when $\gamma > \frac{1}{2}\theta$, the right-hand surface lies in a shadow and the left-hand surface is only partially illuminated. It is easily perceived that the length of surface which is directly illuminated

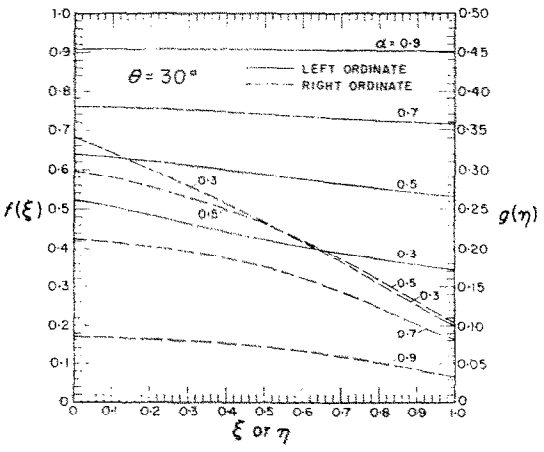

FIG. 3. Local energy-absorption functions for parallel rays entering a 30° V-groove, $\gamma \leqslant \theta/2$.

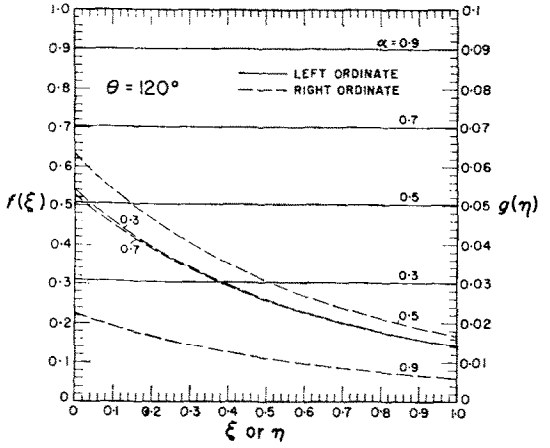

FIG. 4. Local energy-absorption functions for parallel rays entering a 120° V-groove, $\gamma \leqslant \theta/2$.

becomes an additional parameter. To illustrate the nature of the results, numerical consideration has been given to the case wherein the region of direct illumination is $0{\cdot}5 < x/L \leqslant 1$, i.e. half of the left-hand surface of the V. The governing equations (1) may be suitably modified by deleting the term $S \sin[(\theta/2) - \gamma]$ in the second equation and by retaining $S \sin[(\theta/2) + \gamma]$ in the first equation

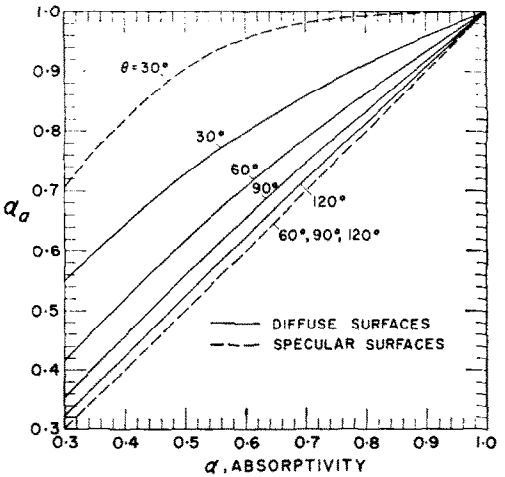

FIG. 5. Apparent absorptivity for parallel rays incident on the region $0{\cdot}5 < X \leqslant 1$ of a V-groove.

only in the range $0{\cdot}5 < x/L \leqslant 1$. Numerical solutions have been carried out for the same θ and α values as before. The energy absorbed in the cavity as a whole may be represented by a_a as defined by equation (4), and this information is given in Fig. 5 by the solid lines. By comparing Figs. 2 and 5, it is seen that the apparent absorptivity is lower in a partially illuminated cavity than in a fully illuminated cavity. Typical results for the local distribution of absorbed energy are presented on Figs. 6 and 7, respectively, for $\theta = 30°$ and 120°. It is seen that the disparity between the energy absorbed on the directly illuminated portion of the surface and that absorbed in other regions diminishes as both θ and α decrease.

PARALLEL RAYS, SPECULAR SURFACES

Fully illuminated surfaces, $\gamma < \frac{1}{2}\theta$

To illustrate the method of approach for specularly reflecting surfaces, consideration may be given to a typical

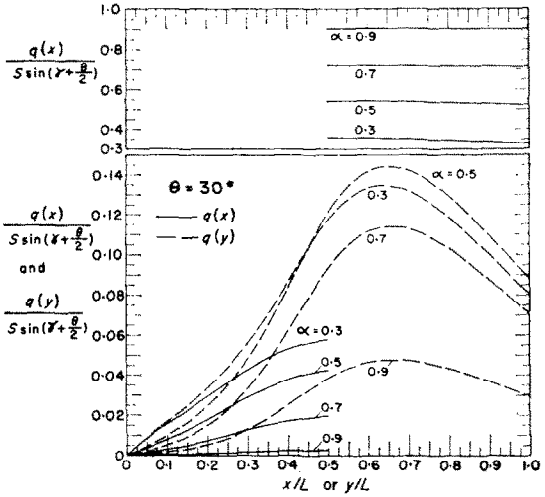

FIG. 6. Absorbed energy distributions for parallel rays incident on the region $0{\cdot}5 < X \leqslant 1$ of a 30° V-groove.

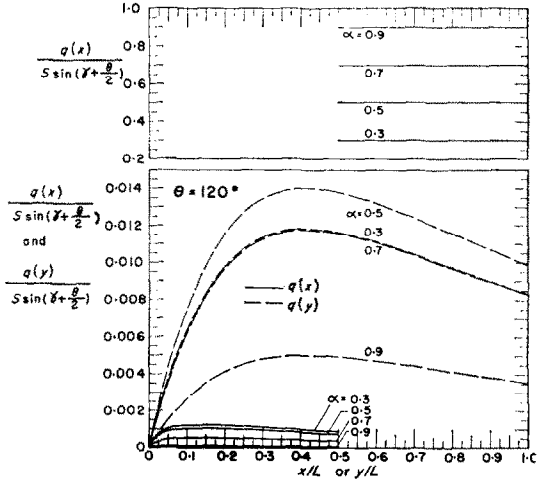

FIG. 7. Absorbed energy distributions for parallel rays incident on the region $0{\cdot}5 < X \leqslant 1$ of a 120° V-groove.

reflection pattern as pictured in Fig. 1(b). Here is shown a particular ray incident at x' which experiences two surface contacts and then leaves the cavity, just grazing the rim. For rays which strike at $x < x'$, there would be three surface contacts, while for rays which strike at $x > x'$, there would be two surface contacts. The initial angle of contact between the surface and the ray is $\gamma + \theta/2$, and this increases by θ for each contact.

In general, a ray approaching the surface for its nth contact makes an angle $\gamma + (n - \frac{1}{2})\theta$ with the surface. To achieve actual contact, it is necessary that $\gamma + (n - \frac{1}{2})\theta < \pi$. From this, it follows that the number of surface contacts n' experienced by rays which initially strike between $x = 0$ and $x = x'$ is equal to the integral part of $[(\pi - \gamma)/\theta + \frac{1}{2}]$*. Rays which initially strike in the region between $x = x'$ and $x = L$ experience $(n' - 1)$ surface contacts. The dividing point x' is determined by using the law of sines as

$$x'/L = X' = \sin[(n' - \tfrac{1}{2})\theta + \gamma] \Big/ \sin\left(\frac{\theta}{2} + \gamma\right). \quad (6)$$

Rays which initially strike the right-hand surface of the V experience a similar reflection pattern. The number of contacts n'' experienced by rays initially incident between $y = 0$ and $y = y''$ is calculated as before, except that γ is replaced by $(-\gamma)$. Additionally, y'' may be found from equation (6) with n' replaced by n'' and γ replaced by $(-\gamma)$.

If a ray experiences n surface contacts, the following fraction of its energy is absorbed:

$$\alpha + \alpha(1 - \alpha) + \alpha(1 - \alpha)^2 + \ldots + \alpha(1 - \alpha)^{n-1} = 1 - (1 - \alpha)^n.$$

With this, and with the foregoing knowledge of the number of surface contacts experienced by rays which strike various portions of the surface, the apparent absorptivity can easily be calculated from its definition, equation (4). After rearrangement, this becomes

$$\alpha_a\left(2\cos\gamma\sin\frac{\theta}{2}\right) = [1 - (1 - \alpha X')(1 - \alpha)^{n'-1}]\sin\left(\frac{\theta}{2} + \gamma\right) + [1 - (1 - \alpha Y'')(1 - \alpha)^{n''-1}]\sin\left(\frac{\theta}{2} - \gamma\right). \quad (7)$$

Equation (7) has been numerically evaluated for the same θ and α values as in the previous cases and the results plotted as dashed curves on Fig. 2. Inspection of the figure reveals that for small opening angles the energy-absorbing capability of a specular cavity is much greater than that of a diffuse cavity. As the opening angle grows larger, the relative advantage of the specular cavity diminishes. For the larger opening angles studied, there are certain γ values at which the diffuse cavity is a superior performer.

Partially illuminated surfaces, $\gamma > \frac{1}{2}\theta$

The foregoing analysis can be modified without difficulty to include the case where no external radiation falls directly on the right-hand surface and only part of left-hand surface is directly illuminated. The analytical details will be omitted here. For purposes of comparison with the diffuse cavity, apparent absorptivity results have been calculated for the case where direct illumination extends over the region $0{\cdot}5 < x/L \leqslant 1$. These are shown as dashed lines in Fig. 5. The curves corresponding to opening angles θ of 60°, 90° and 120° are straight lines given by $\alpha_a = \alpha$. There are no specular multireflections in these cases. For $\theta = 30°$, specular multireflections do occur, and the energy absorption exceeds that of the diffuse cavity.

DIFFUSE INCOMING RADIATION, DIFFUSE SURFACES

For purposes of analysis and without loss of generality, the incoming diffuse radiation may be replaced by a black surface b stretched across the opening and radiating into the cavity. If the incoming stream is characterized by an energy e per unit time and per unit area of the cavity opening, so also will the emissive power of the black surface be e. The integral equations stated in equation (1) may be applied after appropriate modifications are made. First of all, owing to the symmetry of the present situation, $H(x) = H(y)$ when $x = y$, and as a consequence only one integral equation need be used, for instance the first of equations (1). Next, the formerly appearing inhomogeneous term is now replaced by eF_{x-b}, in which F_{x-b} corresponds to interchange between a surface location x and the black surface. Then, by angle-factor algebra, $F_{x-b} = 1 - \int_0^L \mathrm{d}F_{x-y}$. If these modifications are incorporated into the first of equations (1) and if, additionally, a new variable

$$\Lambda = 1 - (1 - \alpha)(H/e)$$

is introduced, there follows

$$\Lambda(x) = \alpha + \rho\int_0^L \Lambda(y)\,\mathrm{d}F_{x-y}. \quad (8)$$

It is easily proven that the solution for Λ can be written as the sum $f(x/L) + g(x/L)$, where f and g are solutions of equation (2). Then, noting that $q = \alpha H$, we have

$$q(x)/e = [\alpha/(1 - \alpha)][1 - f(x/L) - g(x/L)]. \quad (9)$$

Additionally $q(x) = q(y)$ when $x = y$. The over-all absorption of energy is found by carrying out the integrals $\int q(x)\,\mathrm{d}x$ and $\int q(y)\,\mathrm{d}y$. Utilizing the result of this operation and noting that the incoming radiation is expressed as $e[2L\sin\theta/2]$, the apparent absorptivity takes the form

$$\alpha_a = \left(\alpha/(1 - \alpha)\sin\frac{\theta}{2}\right)\left[1 - \int_0^1 f(\xi)\,\mathrm{d}\xi - \int_0^1 g(\eta)\,\mathrm{d}\eta\right]. \quad (10)$$

Numerical results based on the evaluation of equation (10) are presented on Fig. 8. As was previously the case, the greatest deviations of α_a from α occur for small opening angles and low surface absorptivities. By considering Figs. 2, 5 and 8, it is seen that the relative absorbing capabilities of a diffuse cavity either for rays or for diffuse incoming radiation depend upon the inclination angle of the rays.

* If this bracket is precisely equal to an integer, then n' is equal to that integer minus 1.

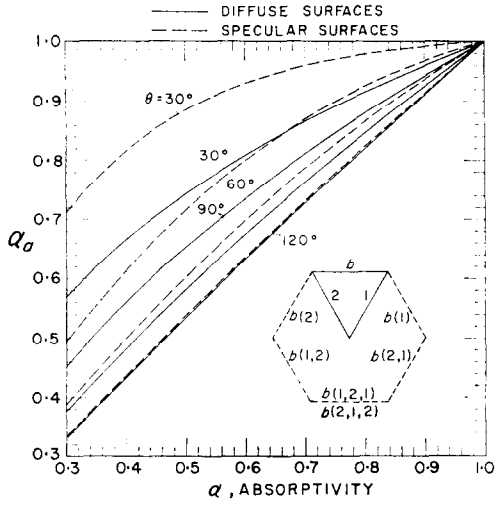

FIG. 8. Apparent absorptivity for diffuse energy incident on a V-groove.

Local energy-absorption results may be calculated from equation (9) in conjunction with Figs. 3 and 4.

DIFFUSE INCOMING RADIATION, SPECULAR SURFACES

If the diffuse incoming radiation is replaced by an equivalent black surface b, there is thus formed a complete enclosure consisting of plane surfaces, two of which are specular reflectors and one of which is black. The radiant interchange within such an enclosure is most conveniently analysed by a newly formulated method of approach that makes use of the images which are formed by the specular surfaces [2].

The over-all energy absorbed within the cavity as a whole is the difference between the incoming radiation and that which streams outward through the fictitious black surface b, i.e.

$$Q = \left[2L \sin \frac{\theta}{2}\right](e - H_b),$$

in which H_b is the reflected radiation incident on b per unit time and area. The apparent absorptivity thus becomes

$$\alpha_a = 1 - (H_b/e). \tag{11}$$

To find the energy incident on surface b, one forms the images of surface b in the mirrors 1 and 2 as illustrated for the 60° V in the inset of Fig. 8. The notation $b(1)$ indicates the image of b formed by mirror 1, $b(1, 2)$ indicates the image of b formed by successive reflections in mirrors 1 and 2, etc. From image $b(1)$, the contribution to H_b is $\rho e F_{b-b(1)}$, in which $F_{b-b(1)}$ is an angle factor for diffuse interchange between surfaces b and $b(1)$. Similar contributions to H_b are made by the other images. Thus, for the illustrative 60° case,

$$H_b/e = 2\rho F_{b-b(1)} + 2\rho^2 F_{b-b(1,2)} + \rho^3 F_{b-b(1,2,1)}. \tag{12}$$

The apparent absorptivity can then be calculated from equation (11) in conjunction with equation (12).

A corresponding calculation has been carried through for the other opening angles under consideration, and the results plotted as dashed lines on Fig. 8. Inspection of the figure shows that, for diffuse incoming energy, a specular cavity is a more efficient absorber than a diffuse cavity. This is especially true at small opening angles and low surface absorptivity.

ACKNOWLEDGEMENTS

This research was sponsored by the National Aeronautics and Space Administration. Technical direction was supplied by Mr. S. Lieblein of the NASA Lewis Research Center.

REFERENCES

1. E. M. SPARROW, J. L. GREGG, J. V. SZEL and P. MANOS, Analysis, results and interpretation for radiation between some simply arranged gray surfaces. *Trans. ASME. J. Heat Transfer* C83, 207–214 (1961).
2. E. M. SPARROW, E. R. G. ECKERT and V. K. JONSSON, An enclosure theory for radiative exchange between specularly and diffusely reflecting surfaces (ASME, paper 61-WA-167). *Trans. ASME J. Heat Transfer*. To be published.